IEEE Access
Multidisciplinary | Rapid Review | Open Access Journal

Received April 5, 2017, accepted May 19, 2017, date of publication June 8, 2017, date of current version June 27, 2017.

Digital Object Identifier 10.1109/ACCESS.2017.2713773

Hierarchical Delay-Dependent Distributed Coordinated Control for DC Ring-Bus Microgrids

CHUNXIA DOU[1,2], DONG YUE[1], (Senior Member, IEEE), ZHANQIANG ZHANG[2], AND JOSEP M. GUERRERO[3], (Fellow, IEEE)

[1]Institute of Advanced Technology, Nanjing University of Posts and Telecommunications, Nanjing 210023, China
[2]Institute of Electrical Engineering, Yanshan University, Qinhuangdao 066004, China
[3]Department of Energy Technology, Aalborg University, 9220 Aalborg, Denmark

Corresponding author: Chunxia Dou (cxdou@ysu.edu.cn)

This work was supported in part by the National Natural Science Foundation of China under Grant 61573300 and Grant 61533010 and in part by the Hebei Provincial Natural Science Foundation of China under Grant E2016203374.

ABSTRACT In this paper, a hierarchical distributed coordinated control method is proposed based on the multi-agent system for dc ring-bus microgrids to improve the bus voltage performance. First, a two-level multi-agent system is built, where each first-level unit control agent is associated with a distributed energy resource to implement local decentralized control, and the second-level control agent is associated with the first-level agent to implement distributed coordination control together with the first-level agent. Afterward, the assessment index of each distributed energy resource subsystem is established. By the assessment index, the multi-agent system can judge whether the subsystem should implement the local decentralized control or the distributed coordinated control. Furthermore, by means of the assessment index, both the local controller and distributed coordinated controller are designed, respectively, based on two kinds of dynamic models of DER unit. To reduce the communication pressure, the distributed coordinated controller is built by local controller combined with the coordinated control laws. The coordinated control laws are synthesized by using the states from only neighboring subsystems. Considering the effect of communication delays on control performance, a delay-dependent H∞ robust control method is proposed to design the distributed coordinated controller. Finally, the validity of the proposed control scheme is testified by simulation results.

INDEX TERMS DC microgrid, multi-agent system, distributed coordinated control, assessment index, decentralized control, delay-dependent.

I. INTRODUCTION

The increasing use of DC distributed energy resources (DERs), such as photovoltaic (PV) panels, fuel cells and storage devices, has motivated growing interest in DC microgrids (MGs) [1], [2]. DC MGs have the following well-known features: (i) The power distribution is more efficient than that in AC MGs, since in DC MGs there is no reactive power; (ii) The power supply for DC loads is more efficient than that in AC MGs. So far, fifty percent of loads of the whole buildings are DC loads [3]. In addition, the development of electric vehicles implies increasing trend of DC demands. In order to meet these DC loads, an AC MG must use a two-stage conversion topology: first AC-DC and then DC-DC. Using a DC MG to supply these DC loads would avoid an unnecessary AC-DC conversion stage, and thus the overall efficiency can be enhanced.

One of the major concerns in DC MGs is how to design a feasible and efficient control scheme to improve the bus voltage performance. So far, many researches had proposed the decentralized ''peer to peer'' control scheme, which means each DER unit is controlled independently by using only local information, such as the local droop control [4], [5]. This control scheme is obviously easy to be implemented. However, it might lead to large dynamic bus voltage deviations between DER subsystems.

In order to solve the problem above, many researches had proposed secondary coordinated controls, which are mainly classified into three categories: centralized communications and control [6]–[8], centralized communication and distributed control [9], [10], and distributed coordinated control [11]–[13]. No matter which secondary coordinated control scheme above is used, the voltage performance of

whole system can be effectively improved. However, the effect of communication delays on control performance has to be considered. Since the first two control schemes depend on global information, communication delays existing in the communication system might pose greater influence on the control performance [14]. In order to reduce the effect of communication delays, the third scheme can be designed by using only distributed information from neighbors.

For the reasons above, on the basis of the authors' previous research regarding DC radial MG [17], the multi-agent system (MAS) based distributed coordinated control method is developed for DC ring-bus MGs in this paper. It is worth mentioning that, in a ring-bus MG, each DER unit might be connected with multiple other DER units rather than only one or two DER units, therefore, the control strategies in this paper are very different from those for a radial MG. The main contributions of this paper can be summarized as follows:

(i) Two-level MAS based distributed coordinated control structure is proposed. Each first-level unit control agent is associated with a DER unit to implement local decentralized control, and then a second-level agent is associated with the unit control agent to implement distributed coordinated control together with the unit control agent. In detail, distributed coordinated control is formed by the coordinated control laws from the second-level agent combining with the local controller of the associated unit control agent. It is worth mentioning that the coordinated control laws are synthesized by using the states from the neighboring second-level agents, so that the communication pressure will be largely reduced.

(ii) As an innovative work, the assessment index of each DER unit is defined with the differential of bus voltage deviation. According to the range of assessment index, the multi-agent system can judge whether the subsystem should implement the local decentralized control or the distributed coordinated control. Furthermore, by means of the assessment index, both the local controller and distributed coordinated controller are designed respectively based on two kinds of dynamic models of DER unit. Considering the effect of communication delays on control performance, the distributed coordinated controller is designed by means of a delay-dependent H_∞ robust control method. Finally, the control performance is testified by means of simulation results.

The rest of this paper is outlined as follows. The MAS based distributed coordinated control scheme is built in Section II. In Section III two kinds of dynamic models are established according to the assessment index. The local decentralized and distributed coordinated controllers are discussed respectively in Section IV. The control performance is verified in Section V. Section VI concludes the paper.

II. MAS BASED DISTRIBUTED COORDINATED CONTROL SCHEME

A DC ring-bus MG example is shown in Fig.1, where each DER unit supplies a local load and a public load connected nearby its bus. When the point of common coupling (PCC) switch between the DC MG and a main grid is disconnected,

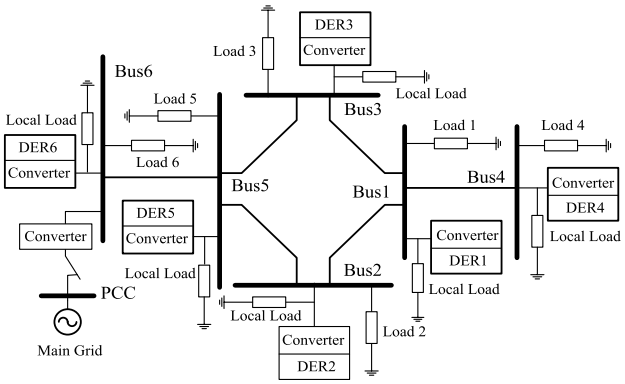

FIGURE 1. Example of a DC ring-bus MG.

the DC ring-bus MG operates in islanded mode. In this case, the two-level MAS is proposed to implement distributed coordinated control. The MAS based distributed coordinated control scheme is depicted in Fig.2.

With respect to the Fig. 2, each first-level unit control agent is designed as a hybrid agent, which is composed of reactive lay and deliberative layer as shown in Fig. 3. The reactive layer defined as "*recognition*, *perception* and *action*", has priority to respond quickly to the emergencies of operation status. The deliberative layer defined as "*belief*, *desire* and *intent* (BDI)", has high intelligence to control the dynamic behavior of its DER unit. The local controller (i.e. *intent*) is determined in the decision making module by means of local knowledge and recognition information (i.e. *belief*), and is implemented by means of the action module (i.e. *desire*).

Each second-level agent is designed as a BDI agent as shown in Fig. 4. First, an assessment index (defined in Section III) is estimated in the recognition module. When the assessment index is larger than a specified threshold, the coordinated control laws (i.e. *intent*) are synthesized in the decision making module by using the knowledge information, as well as the states information exchanged among the neighboring second-level agents (i.e. *belief*). Bridging the interactions among two-level agents, the coordinate control laws are sent to the connected first-level agent, and then are combined with the local decentralized controller to form distributed coordinated controller to implement the distributed coordinated control for the bus voltage (i.e. *desire*).

The interactions among agents are designed as follows: (i) master-slave mode among different levels of agents; (ii) non master-slave mode among the same level of agents. The first one means that the request from a second-level agent must be responded by the asked first-level agent. In other word, the second-level agent has priority over the first-level one. The second one implies that the same level of agents interact in an equal way.

III. DYNAMIC MODELING OF DER UNIT

Corresponding to Fig.1, taking the 1st DER unit as an example, the dynamic model is described as shown in Fig. 5.

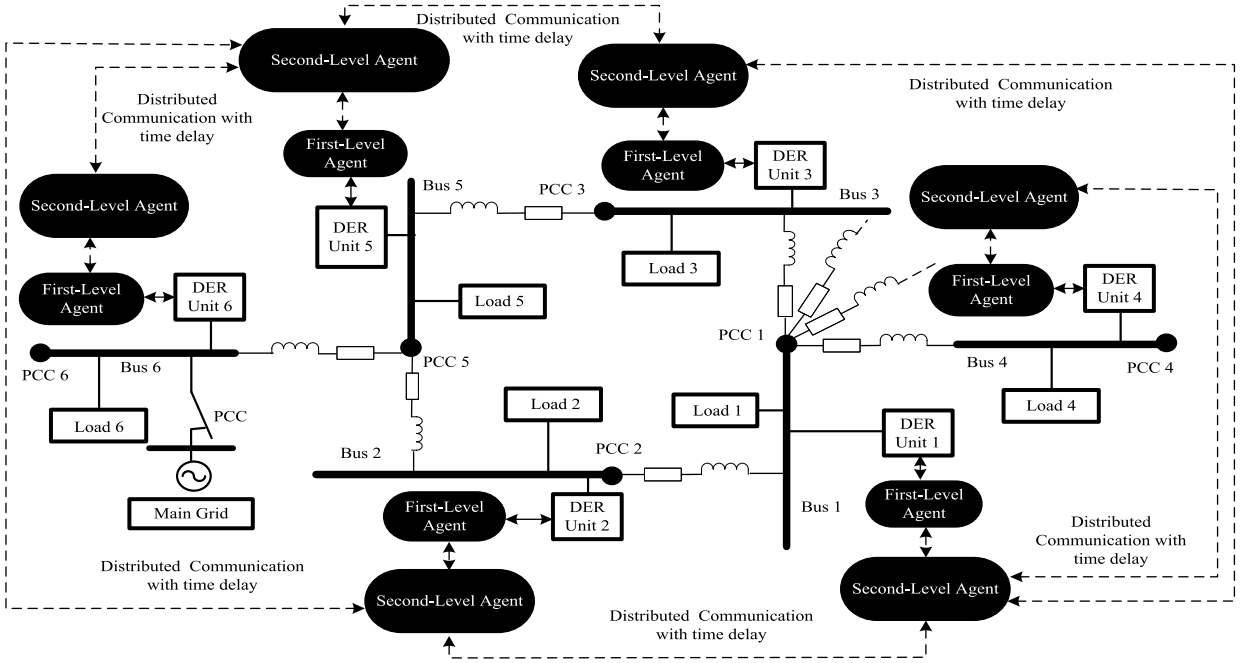

FIGURE 2. MAS based distributed coordinated control scheme.

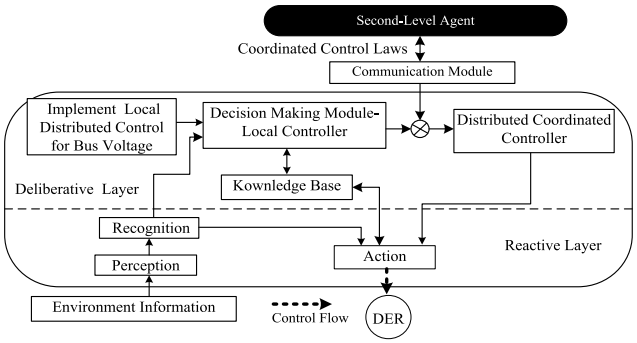

FIGURE 3. Structure of the first-level unit control agent.

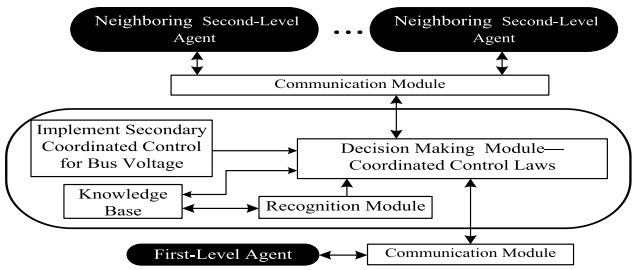

FIGURE 4. Structure of the second-level agent.

Without loss of generality, the 1st DER unit is connected with m-1 DER units through DC lines with different impedances specified by parameters $R1j > 0$ and $L1j > 0, j \in \{2, 3, \cdots m\}$. In the 1st DER unit, a DC/DC buck converter is presented to supply a local load and a public load which are connected to the bus 1 through an LC filter. The local load is usually much smaller than the public load, and thus is regarded as a current disturbance.

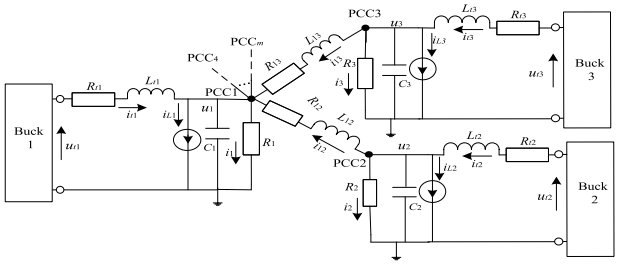

FIGURE 5. Dynamic model of the 1st DER unit.

Corresponding to Fig.5, a set of equations is written as follows:

$$\text{DER1}\begin{cases} \dfrac{du_1}{dt} = -\dfrac{1}{R_1C_1}u_1 + \dfrac{1}{C_1}i_{t1} - \dfrac{1}{C_1}i_{L1} + \dfrac{1}{C_1}\sum_{j=2}^{m} i_{1j} \\ \dfrac{di_{t1}}{dt} = -\dfrac{1}{L_{t1}}u_1 - \dfrac{R_{t1}}{L_{t1}}i_{t1} + \dfrac{1}{L_{t1}}u_{t1} \end{cases} \quad (1)$$

where all parameters and variables are described as shown in Fig. 5.

According to [18], due to i_{1j} is the current between two DC buses, $di_{1j}/dt = -di_{j1}/dt = 0$, and

$$i_{1j} = -i_{j1} = (u_j - u_1)/R_{1j},\ j \in \{2, 3, \cdots, m\}. \quad (2)$$

The actual measurement value of u_1 is given as follows:

$$\hat{u}_1 = \bar{u}_1 + \frac{1}{C_1}\int_0^t \sum_{j=2}^{m} i_{1j}, \quad (3)$$

where $\hat{u}_1$ is the actual measurement value of u_1; $\overline{u}_1$ is the average value of u_1; usually $\overline{u}_1 = u_{ref}$, and u_{ref} is the desired value.

According to (3), the following equation can be obtained:

$$C_1 \frac{d(\hat{u}_1 - u_{ref})}{dt} = \sum_{j=2}^{m} i_{1j}. \tag{4}$$

The sum of currents $\sum_{j=2}^{m} i_{1j}$ in the right side of Eq. (4) can be obtained through the differential of voltage deviation. The differential of voltage deviation can be calculated by using the real-time bus voltage measurement and the desired voltage value of the 1st DER unit. Here, the differential of voltage deviation $d(\hat{u}_1 - u_{ref})/dt$ is defined as the assessment index of the1st DER unit.

Remark 1: If the assessment index $d(\hat{u}_1 - u_{ref})/dt \leq \varepsilon_1$, where ε_1 is a specified threshold, then the sum of currents $\sum_{j=2}^{m} i_{1j}$ in (1) can be treated as a current disturbance, so that the dynamic model of the 1st DER unit can be described as:

$$\text{DER1} : \dot{\boldsymbol{x}}_1(t) = \boldsymbol{A}_1 \boldsymbol{x}_1(t) + \boldsymbol{B}_1 v_1(t) + \boldsymbol{D}_1 \boldsymbol{\omega}_1(t), \tag{5}$$

where $\boldsymbol{x}_1(t) = [u_1(t), i_{t1}(t)]^T$ is the state vector; $v_1(t) = u_{t1}(t)$ is the input variable; $\boldsymbol{\omega}_1(t) = [i_{L1}(t), \sum_{j=2}^{m} i_{1j}(t)]^T$ is the disturbance vector; all the coefficient matrices are expressed as follows:

$$\boldsymbol{A}_1 = \begin{bmatrix} -1/R_1C_1 & 1/C_1 \\ -1/L_{t1} & -R_{t1}/L_{t1} \end{bmatrix}; \quad \boldsymbol{B}_1 = \begin{bmatrix} 0 \\ 1/L_{t1} \end{bmatrix};$$
$$\boldsymbol{D}_1 = \begin{bmatrix} -1/C_1 & 1/C_1 \\ 0 & 0 \end{bmatrix}.$$

Since there is no coupling term in (5), the 1st DER unit can be stabilized only by its local controller in the first-level unit control agent. The local controller design will be discussed in Subsection IV. A.

Remark 2: If the assessment index $d(\hat{u}_1 - u_{ref})/dt > \varepsilon_1$, then the sum of currents $\sum_{j=2}^{m} i_{1j}$ in (1) is no longer regarded as a current disturbance. In this case, taking into account the communication delays, the dynamic model of the 1st DER unit can be rewritten as:

$$\text{DER1} : \dot{\boldsymbol{x}}_1(t) = \tilde{\boldsymbol{A}}_1 \boldsymbol{x}_1(t) + \boldsymbol{B}_1 v_1(t) + \sum_{j=2}^{m} \boldsymbol{A}_{1j} \boldsymbol{x}_j(t - \tau_{1j}) + \tilde{\boldsymbol{D}}_1 \boldsymbol{\omega}_1(t), \tag{6}$$

where $\boldsymbol{x}_j(t - \tau_{1j}) = [u_j(t - \tau_{1j}), i_{tj}(t - \tau_{1j})]^T$ is the state information from the jth to the 1st second-level agent with communication delays, and $\tau_{1j} \leq \bar{\tau}, (\bar{\tau} > 0)$ are the communication delays between the 1st and the jth second-level agents;

$$\tilde{\boldsymbol{A}}_1 = \begin{bmatrix} -1/R_1C_1 - \sum_{j=2}^{m} 1/R_{1j}C_1 & 1/C_1 \\ -1/L_{t1} & -R_{t1}/L_{t1} \end{bmatrix};$$
$$\boldsymbol{A}_{1j} = \begin{bmatrix} 1/R_{1j}C_1 & 0 \\ 0 & 0 \end{bmatrix}; \quad \tilde{\boldsymbol{D}}_1 = \begin{bmatrix} -1/C_1 & 0 \\ 0 & 0 \end{bmatrix}.$$

Except the vector and matrices above, other are the same as (5).

Since there is the coupling effects among the 1st DER unit and the jth DER in (6) ($j \in \{2, 3, \cdots, m\}$), the 1st DER unit need be regulated by means of the distributed coordinated controller. The distributed coordinated controller design will be discussed in Subsection IV.B.

For designing the distributed coordinated controller, besides the dynamic model of the 1st DER unit, the dynamic model of the jth DER unit $j \in \{2, 3, \cdots, m\}$ also needs to be described.

Remark 3: If the assessment index $d(\hat{u}_1 - u_{ref})/dt > \varepsilon_1$, when building the dynamic model of the jth DER unit, the current $i_{j1} = -i_{1j}$ between the 1st DER unit and the jth DER unit cannot be regarded as a current disturbance. Except the current, the sum of other currents $\sum_{k \in \Omega_j, k \neq 1} i_{jk}$, where Ω_j is set of the DER units connected to the jth DER unit, might be regarded as a current disturbance. In this case, the dynamic model of the jth DER unit can be described as:

$$\text{DER } j : \dot{\boldsymbol{x}}_j(t) = \tilde{\boldsymbol{A}}_j \boldsymbol{x}_j(t) + \boldsymbol{B}_j v_j(t) + \boldsymbol{A}_{j1} \boldsymbol{x}_1(t - \tau_{1j}) + \tilde{\boldsymbol{D}}_j \boldsymbol{\omega}_j(t), \quad j \in \{2, 3, \cdots, m\}, \tag{7}$$

where $\boldsymbol{x}_j(t) = \left[u_j(t), i_{tj}(t)\right]^{\mathrm{T}}$ is the state vector; $v_j(t) = u_{tj}(t)$ is the input variable; $\boldsymbol{\omega}_j(t) = [i_{Lj}(t), \sum_{k \neq 1}^{ijk}(t)]^T$ is the disturbance vector; $\boldsymbol{x}_1(t - \tau_{1j}) = [u_1(t - \tau_{1j}), i_{t1}(t - \tau_{1j})]^T$ is the state vector with communication delays from the 1st to the jth second-level agent; the coefficient matrices is expressed as follows:

$$\tilde{\boldsymbol{A}}_j = \begin{bmatrix} -1/R_jC_j - 1/R_{1j}C_j & 1/C_j \\ -1/L_{tj} & -R_{tj}/L_{tj} \end{bmatrix}; \quad \boldsymbol{B}_j = \begin{bmatrix} 0 \\ 1/L_{tj} \end{bmatrix};$$
$$\boldsymbol{A}_{j1} = \begin{bmatrix} 1/R_{1j}C_j & 0 \\ 0 & 0 \end{bmatrix}; \quad \tilde{\boldsymbol{D}}_j = \begin{bmatrix} -1/C_j & 1/C_j \\ 0 & 0 \end{bmatrix}.$$

The control objective of both the local and distributed coordinated controllers is to guarantee that the state variables (voltage and current) track their desired trajectories, and then achieving the desired dynamic performances. Therefore, a reference model is given for tracking control of the 1st DER unit as follows:

$$\dot{\boldsymbol{x}}_{r1}(t) = \boldsymbol{A}_{r1} \boldsymbol{x}_{r1}(t), \tag{8}$$

where $\boldsymbol{x}_{r1}(t)$ represents the desired trajectory for $\boldsymbol{x}_1(t)$; $\boldsymbol{A}_{r1}$ is a specific asymptotically stable matrix.

The reference model of the jth DER unit can be expressed as:

$$\dot{\boldsymbol{x}}_{rj}(t) = \boldsymbol{A}_{rj} \boldsymbol{x}_{rj}(t), j \in \{2, 3, \cdots, m\}, \tag{9}$$

where $\boldsymbol{x}_{rj}(t)$ represents the desired trajectory for $\boldsymbol{x}_j(t)$; $\boldsymbol{A}_{rj}$ is also a specific asymptotically stable matrix.

IV. DISTRIBUTED COORDINATED CONTROL STRATEGIES

A. FIRST-LEVEL LOCAL CONTROLLER DESIGN

When the assessment index $d(\hat{u}_1 - u_{ref})/dt \leq \varepsilon_1$, the first-level unit control agent implements local distributed control (i.e. control mode 1) for the 1st DER unit.

The local controller is designed as:

$$v_1(t) = \boldsymbol{K}_1 [\boldsymbol{x}_1(t) - \boldsymbol{x}_{r1}(t)], \tag{10}$$

where $\boldsymbol{K}_1$ is the parameter matrix of the local controller.

Combining Eq.(5) with Eq.(8), the tracking control system of the 1st DER unit under the local controller in (10) is written as:

$$\text{DER1}: \dot{\hat{\boldsymbol{x}}}_1(t) = \hat{\boldsymbol{A}}_1\hat{\boldsymbol{x}}_1(t) + \hat{\boldsymbol{D}}_1\boldsymbol{\omega}_1(t), \tag{11}$$

where $\hat{\boldsymbol{x}}_1(t) = \left[\boldsymbol{x}_1^T(t), \boldsymbol{x}_{r1}^T(t)\right]^{\mathrm{T}}$; $\hat{\boldsymbol{A}}_1 = \begin{bmatrix} \boldsymbol{A}_1 + \boldsymbol{B}_1\boldsymbol{K}_1 & -\boldsymbol{B}_1\boldsymbol{K}_1 \\ 0 & \boldsymbol{A}_{r1} \end{bmatrix}$; $\hat{\boldsymbol{D}}_1 = \begin{bmatrix} \boldsymbol{D}_1 \\ 0 \end{bmatrix}$.

For the purpose of robust control, H_∞ control performance regarding the tracking error is given as follows [19], [20]:

$$\int_0^{t_f} [(\boldsymbol{x}_1(t) - \boldsymbol{x}_{r1}(t))^T \boldsymbol{Q}_1 (\boldsymbol{x}_1(t) - \boldsymbol{x}_{r1}(t))]dt \Big/ \int_0^{t_f} \boldsymbol{\omega}_1(t)^T\boldsymbol{\omega}_1(t)dt \le \rho_1^2, \tag{12}$$

where t_f denotes terminal time of control; $\boldsymbol{Q}_1 = \boldsymbol{Q}_1^T > 0$ is weighting matrix.

The physical meaning of (12) is that effect of $\forall\boldsymbol{\omega}_1(t)$ on the tracking error $\boldsymbol{x}_1(t) - \boldsymbol{x}_{r1}(t)$ must be attenuated below a desire level ρ_1 from the energy viewpoint.

Considering the initial conditions, the H_∞ control performance is rewritten as:

$$\int_0^{t_f} \hat{\boldsymbol{x}}_1^T(t)\hat{\boldsymbol{Q}}_1\hat{\boldsymbol{x}}_1(t)dt \le \rho_1^2 \int_0^{t_f} \boldsymbol{\omega}_1^T(t)\boldsymbol{\omega}_1(t)dt + \boldsymbol{x}_1^T(0)\boldsymbol{P}_1\hat{\boldsymbol{x}}_1(0), \tag{13}$$

where $\hat{\boldsymbol{Q}}_1 = \begin{bmatrix} \boldsymbol{Q}_1 & -\boldsymbol{Q}_1 \\ -\boldsymbol{Q}_1 & \boldsymbol{Q}_1 \end{bmatrix}$; $\boldsymbol{P}_1 = \boldsymbol{P}_1^T > 0$ is the weighting matrix.

According to the following Theorem 4.1, the first-level unit control agent can determine the local controller for the 1st DER unit.

Theorem 1: The tracking control system (11) is asymptotically stable with the guaranteed H_∞ control performance in (13) for $\forall\boldsymbol{\omega}_1(t)$, if there exists $\boldsymbol{P}_1 = \boldsymbol{P}_1^T > 0$ satisfying the following matrix inequality

$$\begin{bmatrix} \hat{\boldsymbol{A}}_1^T\boldsymbol{P}_1 + \boldsymbol{P}_1\hat{\boldsymbol{A}}_1 + \hat{\boldsymbol{Q}}_1 & \boldsymbol{P}_1\hat{\boldsymbol{D}}_1 \\ \hat{\boldsymbol{D}}_1^T\boldsymbol{P}_1 & -\rho_1^2\boldsymbol{I} \end{bmatrix} \le 0. \tag{14}$$

The proof is given in Appendix A

The inequality (14) is not a linear matrix inequality (LMI). Thus it needs to be transformed into LMI according to the following procedures:

(1) Denote a new matrix

$$\boldsymbol{W}_1 = \begin{bmatrix} \overline{\boldsymbol{W}}_1 & 0 \\ 0 & \boldsymbol{I} \end{bmatrix} = \begin{bmatrix} \boldsymbol{P}_1^{-1} & 0 \\ 0 & \boldsymbol{I} \end{bmatrix},$$

where $\overline{\boldsymbol{W}}_1^T = \overline{\boldsymbol{W}}_1 = \boldsymbol{P}_1^{-1} > 0$. Left and right multiplying the matrix above into the inequality (14), it can be obtained that

$$\begin{bmatrix} \overline{\boldsymbol{W}}_1\hat{\boldsymbol{A}}_1^T + \hat{\boldsymbol{A}}_1\overline{\boldsymbol{W}}_1 + \overline{\boldsymbol{W}}_1\hat{\boldsymbol{Q}}_1\overline{\boldsymbol{W}}_1 & \hat{\boldsymbol{D}}_1 \\ \hat{\boldsymbol{D}}_1^T & -\rho_1^2\boldsymbol{I} \end{bmatrix} \le 0. \tag{15}$$

(2) Define $\overline{\boldsymbol{W}}_1 = \begin{bmatrix} \overline{\boldsymbol{W}}_{11} & 0 \\ 0 & \overline{\boldsymbol{W}}_{11} \end{bmatrix} = \begin{bmatrix} \boldsymbol{P}_{11}^{-1} & 0 \\ 0 & \boldsymbol{P}_{11}^{-1} \end{bmatrix}$, $\hat{\boldsymbol{K}}_1 = \boldsymbol{K}_1\overline{\boldsymbol{W}}_{11}$, $\breve{\boldsymbol{Q}}_1 = \overline{\boldsymbol{W}}_1\boldsymbol{Q}_1\overline{\boldsymbol{W}}_1$, then it is easy to deduce that the inequality (15) is equivalent to LMI.

Remark 4: According to Theorem 4.1, the local controller design can be transformed into the following LMI convex optimization problem:

$$\begin{aligned} &\min_{\overline{W}_{11},\ \hat{K}_1} \rho_1^2, \\ &\text{subject to } \overline{\boldsymbol{W}}_{11} = \overline{\boldsymbol{W}}_{11}^T > 0 \text{ and (15).} \end{aligned} \tag{16}$$

By means of solving the LMI convex optimization problem above, the local controller parameter and H_∞ control performance can be obtained.

B. MAS BASED DISTRIBUTED COORDINATED CONTROL DESIGN

When the assessment index $d(\hat{u}_1 - u_{ref})/dt > \varepsilon_1$, the two-level multi-agents implement the distributed coordinated control together (i.e. control mode 2) for the 1st DER unit.

The distributed coordinated controller is designed as:

$$v_1(t) = \tilde{\boldsymbol{K}}_1[\boldsymbol{x}_1(t) - \boldsymbol{x}_{r1}(t)] + \sum_{j=2}^{m} \tilde{\boldsymbol{K}}_{1j}\boldsymbol{x}_j(t - \tau_{1j}), \tag{17}$$

where $\tilde{\boldsymbol{K}}_1$ is the parameter matrix of local controller; $\tilde{\boldsymbol{K}}_{1j}$ is the parameter matrix of coordinated control law from the jth to the 1st second-level agent, $j \in \{2, 3, \cdots, m\}$.

Combining Eq. (6) with Eq. (8), the tracking control system of the 1st DER unit under the distributed coordinated controller (17) is written as follows:

$$\text{DER1}: \dot{\hat{\boldsymbol{x}}}_1(t) = \overline{\boldsymbol{A}}_1\hat{\boldsymbol{x}}_1(t) + \sum_{j=2}^{m} \overline{\boldsymbol{A}}_{1j}\boldsymbol{x}_j(t - \tau_{1j}) + \overline{\boldsymbol{D}}_1\boldsymbol{\omega}_1(t), \tag{18}$$

where $\hat{\boldsymbol{x}}_1(t) = \left[\boldsymbol{x}_1^T(t), \boldsymbol{x}_{r1}^T(t)\right]^{\mathrm{T}}$;

$$\overline{\boldsymbol{A}}_1 = \begin{bmatrix} \tilde{\boldsymbol{A}}_1 + \boldsymbol{B}_1\tilde{\boldsymbol{K}}_1 & -\boldsymbol{B}_1\tilde{\boldsymbol{K}}_1 \\ 0 & \boldsymbol{A}_{r1} \end{bmatrix}; \quad \overline{\boldsymbol{A}}_{1j} = \begin{bmatrix} \boldsymbol{A}_{1j} + \boldsymbol{B}_1\tilde{\boldsymbol{K}}_{1j} \\ 0 \end{bmatrix};$$

$$\overline{\boldsymbol{D}}_1 = \begin{bmatrix} \tilde{\boldsymbol{D}}_1 \\ 0 \end{bmatrix}.$$

With respect to the jth DER unit, the distributed coordinated controller between the 1st DER unit and the jth DER unit is designed as:

$$v_j(t) = \tilde{\boldsymbol{K}}_j[\boldsymbol{x}_j(t) - \boldsymbol{x}_{rj}(t)] + \tilde{\boldsymbol{K}}_{j1}\boldsymbol{x}_1(t - \tau_{1j}) \tag{19}$$

where $\tilde{\boldsymbol{K}}_j$ is the parameter matrix of local controller of the jth DER unit; $\tilde{\boldsymbol{K}}_{j1}$ is the parameter matrix of coordinated control law from the 1st to the jth second-level agent.

Combining Eq. (7) with Eq. (9), the tracking control system of the jth DER unit under the distributed coordinated controller (19) is given as follows:

$$\begin{aligned} \text{DER}j: \dot{\hat{\boldsymbol{x}}}(t) = \overline{\boldsymbol{A}}_j\hat{\boldsymbol{x}}_j(t) + \overline{\boldsymbol{A}}_{j1}\boldsymbol{x}_1(t - \tau_{1j}) + \overline{\boldsymbol{D}}_j\boldsymbol{\omega}_j(t), \\ j \in \{2, 3, \cdots, m\}, \end{aligned} \tag{20}$$

where $\hat{\boldsymbol{x}}_j(t) = [\boldsymbol{x}_j^T(t), \boldsymbol{x}_{rj}^T(t)]^T$;

$$\overline{\boldsymbol{A}}_j = \begin{bmatrix} \tilde{\boldsymbol{A}}_j + \boldsymbol{B}_j\tilde{\boldsymbol{K}}_j & -\boldsymbol{B}_j\tilde{\boldsymbol{K}}_j \\ 0 & \boldsymbol{A}_{rj} \end{bmatrix}; \quad \overline{\boldsymbol{A}}_{j1} = \begin{bmatrix} \boldsymbol{A}_{j1} + \boldsymbol{B}_j\tilde{\boldsymbol{K}}_{j1} \\ 0 \end{bmatrix};$$

$$\overline{\boldsymbol{D}}_j = \begin{bmatrix} \tilde{\boldsymbol{D}}_j \\ 0 \end{bmatrix}.$$

Combining Eq. (18) with Eq. (20), the augmented system is described as:

$$\text{Inte DER1}: \dot{\tilde{x}}(t) = \tilde{A}\tilde{x}(t) + \widehat{A}\tilde{x}(t\text{-}\tau_{ik}) + \tilde{D}\tilde{\omega}(t) \quad (21)$$

where $\tilde{\boldsymbol{x}}(t) = \left[\boldsymbol{x}_1^T(t), \boldsymbol{x}_{r1}^T(t), \boldsymbol{x}_2^T(t), \boldsymbol{x}_{r2}^T(t), \cdots, \boldsymbol{x}_m^T(t), \boldsymbol{x}_{rm}^T(t)\right]^{\mathrm{T}}$ is the state vector of the augmented system; $\tilde{\boldsymbol{\omega}}(t) = \left[\boldsymbol{\omega}_1^T(t), \boldsymbol{\omega}_2^T(t), \cdots, \boldsymbol{\omega}_m^T(t)\right]^T$ is the disturbance vector; $i \neq k \in \{1, 2, \cdots, m\}$ and $\tau_{ik} = \tau_{ki} \leq \bar{\tau}, \bar{\tau} > 0$;

$$\tilde{\boldsymbol{A}} = \begin{bmatrix} \overline{\boldsymbol{A}}_1 & 0 & \cdots & 0 \\ 0 & \overline{\boldsymbol{A}}_2 & 0 & 0 \\ \vdots & 0 & \ddots & 0 \\ 0 & 0 & 0 & \overline{\boldsymbol{A}}_m \end{bmatrix}; \widehat{\boldsymbol{A}} = \begin{bmatrix} 0 & \overline{\boldsymbol{A}}_{12} & \cdots & \overline{\boldsymbol{A}}_{1m} \\ \overline{\boldsymbol{A}}_{21} & 0 & 0 & 0 \\ \vdots & 0 & \ddots & 0 \\ \overline{\boldsymbol{A}}_{m1} & 0 & 0 & 0 \end{bmatrix};$$

$$\tilde{\boldsymbol{D}} = \begin{bmatrix} \overline{\boldsymbol{D}}_1 & 0 & \cdots & 0 \\ 0 & \overline{\boldsymbol{D}}_2 & 0 & 0 \\ \vdots & 0 & \ddots & 0 \\ 0 & 0 & 0 & \overline{\boldsymbol{D}}_m \end{bmatrix}.$$

Corresponding to the augmented system (21), H_∞ control performance can be rewritten as follows:

$$\int_0^{t_f} \tilde{\boldsymbol{x}}^T(t)\tilde{\boldsymbol{Q}}\tilde{\boldsymbol{x}}(t)dt \leq \rho^2 \int_0^{t_f} \tilde{\boldsymbol{\omega}}^T(t)\tilde{\boldsymbol{\omega}}(t)dt + \mathrm{V}(0), \quad (22)$$

where $\tilde{\boldsymbol{Q}} = \begin{bmatrix} \hat{\boldsymbol{Q}}_1 & 0 & \cdots & 0 \\ 0 & \hat{\boldsymbol{Q}}_2 & 0 & 0 \\ \vdots & 0 & \ddots & 0 \\ 0 & 0 & 0 & \hat{\boldsymbol{Q}}_m \end{bmatrix}; \hat{\boldsymbol{Q}}_i = \begin{bmatrix} \boldsymbol{Q}_i & -\boldsymbol{Q}_i \\ -\boldsymbol{Q}_i & \boldsymbol{Q}_i \end{bmatrix}; i \in \{1, 2, \cdots, m\}$;

V(0) is Lyapunov function initial value.

According to the following Theorem 4.2, the two-level multi-agents can determine the distributed-coordinated controller for the 1st DER unit.

*Theorem 2:*Given allowable upper bound $\bar{\tau}$ of the communication delays, the controlled augmented system (21) is asymptotically stable with the H_∞ control performance in (22) for all communication delays satisfying $\tau_{ik} \in [0, \bar{\tau}]$, if there exist symmetric positive definite matrices $\boldsymbol{P}, \boldsymbol{S}, \boldsymbol{Z}, \boldsymbol{X}$ satisfying the following matrix inequalities

$$\begin{bmatrix} \Theta & \boldsymbol{P}\widehat{\boldsymbol{A}} - \boldsymbol{Y} & \boldsymbol{P}\tilde{\boldsymbol{D}} & \tilde{\boldsymbol{A}}^T\boldsymbol{Z} \\ * & -\boldsymbol{S} & 0 & \widehat{\boldsymbol{A}}^T\boldsymbol{Z} \\ * & * & -\rho^2 & \tilde{\boldsymbol{D}}^T\boldsymbol{Z} \\ * & * & * & -\frac{1}{\bar{\tau}}\boldsymbol{Z} \end{bmatrix} \leq 0, \quad (23)$$

$$\text{and} \begin{bmatrix} \boldsymbol{X} & \boldsymbol{Y} \\ \boldsymbol{Y}^T & \boldsymbol{Z} \end{bmatrix} \geq 0, \quad (24)$$

where, $\Theta = \tilde{\boldsymbol{Q}} + \boldsymbol{S} + \boldsymbol{P}\tilde{\boldsymbol{A}} + \tilde{\boldsymbol{A}}^T\boldsymbol{P} + \bar{\tau}\boldsymbol{X} + \boldsymbol{Y} + \boldsymbol{Y}^T$.

The proof is given in the Appendix B.

The inequality (23) is not a LMI, and thus also needs to be transformed into LMI according to the following procedures:

1) Left and right sides of the inequality (23) multiply by the matrix $diag\left\{\boldsymbol{P}^{-1}, \boldsymbol{I}, \boldsymbol{I}, \boldsymbol{Z}^{-1}\right\}$.

2) Define $\boldsymbol{P}^{-1} = \begin{bmatrix} \bar{\boldsymbol{P}}_1^{-1} & 0 & \cdots & 0 \\ 0 & \bar{\boldsymbol{P}}_1^{-1} & 0 & 0 \\ \vdots & 0 & \ddots & 0 \\ 0 & 0 & 0 & \bar{\boldsymbol{P}}_1^{-1} \end{bmatrix}, \bar{\boldsymbol{P}}_1 = \bar{\boldsymbol{P}}_1^T = \begin{bmatrix} \boldsymbol{P}_1 & 0 \\ 0 & \boldsymbol{P}_1 \end{bmatrix} > 0,$

$\hat{\boldsymbol{K}}_i = \tilde{\boldsymbol{K}}_i\boldsymbol{P}_1^{-1}, \hat{\boldsymbol{K}}_{ik} = \tilde{\boldsymbol{K}}_{ik}\boldsymbol{P}_1^{-1}, \tilde{\boldsymbol{X}} = \boldsymbol{P}^{-1}\boldsymbol{X}\boldsymbol{P}^{-1}, \tilde{\boldsymbol{S}} = \boldsymbol{P}^{-1}\boldsymbol{S}\boldsymbol{P}^{-1}, \widehat{\boldsymbol{Q}} = \boldsymbol{P}^{-1}\tilde{\boldsymbol{Q}}P^{-1}, \tilde{\boldsymbol{Y}} = \boldsymbol{P}^{-1}\boldsymbol{Y}\boldsymbol{P}^{-1}, i \neq k \in \{1, 2, \cdots, m\}$, then it is easy to deduce that the inequality (23) is equivalent to the following LMI:

$$\begin{bmatrix} \tilde{\Theta} & \widehat{\boldsymbol{A}} - \boldsymbol{P}^{-1}\boldsymbol{Y} & \tilde{\boldsymbol{D}} & \boldsymbol{P}^{-1}\tilde{\boldsymbol{A}}^T \\ * & -\boldsymbol{S} & 0 & \widehat{\boldsymbol{A}}^T \\ * & * & -\rho^2 & \tilde{\boldsymbol{D}}^T \\ * & * & * & -\frac{1}{\bar{\tau}}\boldsymbol{Z}^{-1} \end{bmatrix} \leq 0 \quad (25)$$

where $\tilde{\Theta} = \widehat{\boldsymbol{Q}} + \tilde{\boldsymbol{S}} + \tilde{\boldsymbol{A}}P^{-1} + \boldsymbol{P}^{-1}\tilde{\boldsymbol{A}}^T + \bar{\tau}\tilde{\boldsymbol{X}} + \tilde{\boldsymbol{Y}} + \tilde{\boldsymbol{Y}}^T$.

Remark 5: According to Theorem 4.2, the distributed coordinated controller design is transformed into the following LMI convex optimization problem:

$$\begin{aligned} &\min_{P^{-1}, \tilde{K}_1, \cdots, \tilde{K}_m, \tilde{K}_{12}, \cdots, \tilde{K}_{1m}, \tilde{K}_{21}, \cdots, \tilde{K}_{m1}} \rho^2, \\ &\text{subject to } \boldsymbol{P}^{-1} = \boldsymbol{P}^{-T} > 0, (24) \text{ and } (25). \end{aligned} \quad (26)$$

The distributed coordinated controller parameters, allowable maximum upper bound of communication delays and the H_∞ control performance can be obtained by means of solving the above LMI convex optimization problem.

C. IMPLEMENTATION OF THE DISTRIBUTED COORDINATED CONTROL BASED ON MAS

Each DER unit in the DC ring-bus MG (here take the 1st DER unit as an example) can be regulated by using two kinds of control modes. Control mode 1 (i.e. the local control) is implemented by the first-level unit control agent. Control mode 2 (i.e. the distributed coordinated control) is executed by means of the two-level MAS. The implementation flowchart of the two kinds of control modes by means of BDI agents is shown in Fig. 6.

To implement the two kinds of control modes, the interactions among two-level agents are described in Fig.7. In step 1: (i) the second-level agent 1 (SLA1) firstly synthesizes the coordinated control laws by using the states from the neighboring SLAs through non master-slave interactions, i.e. QUERY, INFORM, REQUEST, RESPONSE; (ii) the SLA1 REQUESTs sending the coordinated control laws to its first-level agent 1 (FLA1) through master-slave interaction; (iii) the FLA1 gives RESPONSE to receive the coordinated control laws. Afterwards it will combine the coordinated control laws with the local decentralized

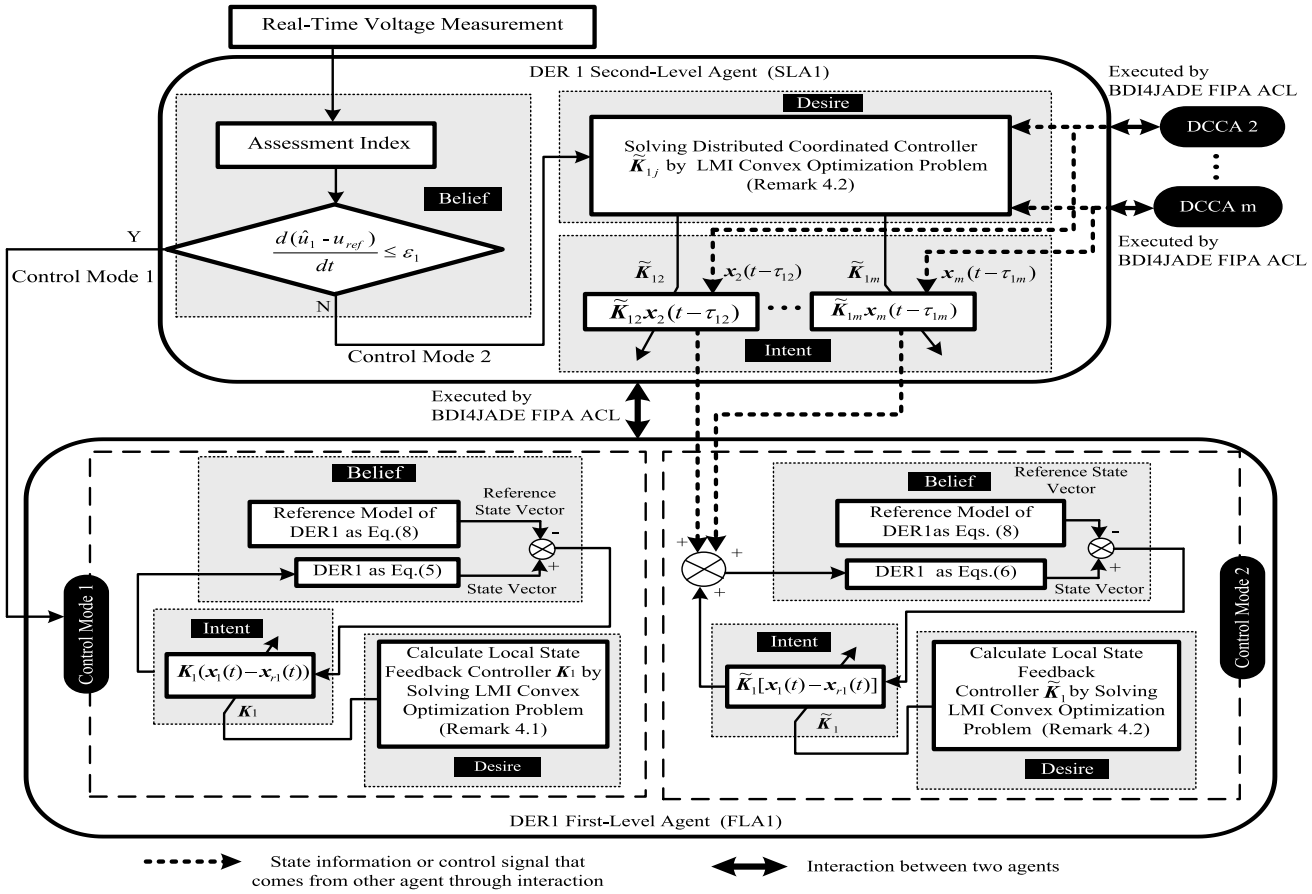

FIGURE 6. Implementation flowchart of two kinds of control modes.

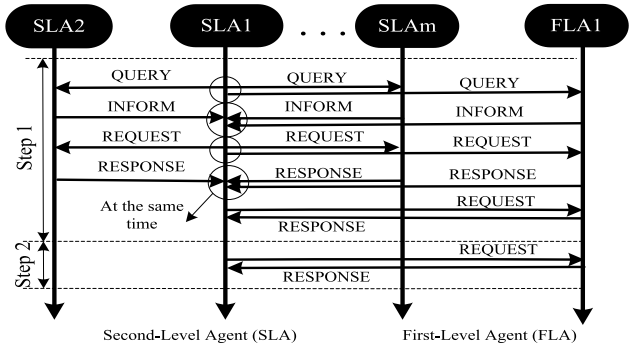

FIGURE 7. Interactions among agents.

controller to implement the control mode 2. In step 2: (i) the SLA1 REQUESTs its FLA1 to implement control mode 1 through master-slave interaction; (ii) the FLA1 gives RESPONSE. The interaction is executed by means of the foundation for intelligent physical agents, agent communication language (FIPA-ACL) in BDI4 Java agent development framework (JADE). BDI4JADE consists of a BDI layer implemented on top of JADE. FIPA-ACL messages are characterized by performative, conversation ID, content and receivers.

V. SIMULATION STUDIES

In order to evaluate the performance of the proposed MAS based distributed coordinated control, four Cases are considered as follows: Case 1: large load changes; Case 2: a short circuit fault; Case 3: different communication delays; Case 4: a communication failure. Furthermore, in the first three Cases, the proposed MAS based distributed coordinated control is compared with a distributed control based on improved droop characteristic [11].

A. CASE 1

The communication delay is assumed as $\tau_{12} = 200ms$. Moreover, the load demand on the bus1 increases twice at $t = 2$s, at the same time, the load demand on the bus2 decreases half. The two load changes result in a large transient voltage deviation between bus1 and bus2. According to their assessment indexes, the DER 1 and DER 2 units need to execute the distributed coordinated control by means of the two-level agents. According to Remark 4.2, by using LMI convex optimization technique in MATLAB toolbox, it can be found that the system is asymptotically stable for any communication delay satisfying $0 \leq \bar{\tau} \leq 3.0978s$. For the purpose of comparison with local control, Figs. 8(a) and (b) firstly give the control performance regarding bus1 and bus2 voltages in the

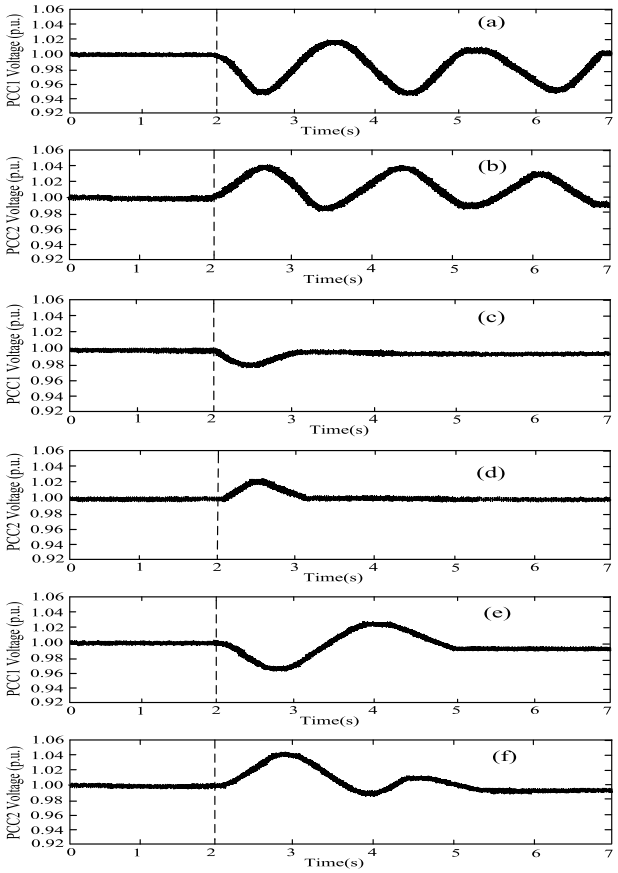

FIGURE 8. Control performance of bus voltages in Case 1. (a) bus1 voltage in the control mode 1; (b) bus2 voltage in the control mode 1; (c) bus1 voltage in the control mode 2; (d) bus2 voltage in the control mode 2; (e) bus1 voltage under the distributed control [11]; (f) bus2 voltage under the distributed control [11].

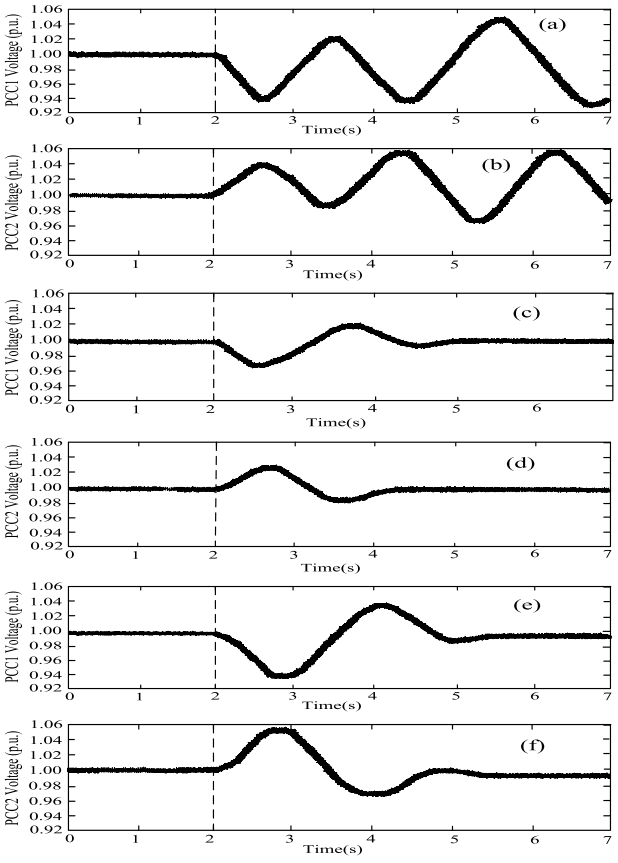

FIGURE 9. Control performance of bus voltages in Case 2. (a) bus1 voltage in control mode 1; (b) bus2 voltage in control mode 1; (c) bus1 voltage in control mode 2; (d) bus2 voltage in control mode 2; (e) bus1 voltage under the distributed control [11]; (f) bus2 voltage under the distributed control [11].

control mode 1. By means of the proposed control mode 2, the control performance is shown in Figs.8(c) and (d). Figs. 8(e) and (f) show the control performance in the compared distributed control [11].

From Figs. 8(a) and (b), it can be seen that by using only the local controller in the first-level unit control agent, without the coordinated control laws from the second-level agents, the two bus voltages have larger fluctuations, and ultimately are not settled down. From Figs.8(c) and (d), it can be observed that, be means of the proposed control mode 2, the two bus voltages present a smaller fluctuation during the period of 2s to 3s, afterwards, are rapidly restored to the desired value (i.e. 1 p.u.) almost without deviation. Figs. 8(e) and (f) show that, when using the compared distributed control [11], the two bus voltages have larger fluctuations on the initial stage of load changes, so that it takes a longer time to stabilize them. The simulation results above indicate that the proposed distributed coordinated control approach ensures the best bus voltage control performance following the load changes.

B. CASE 2

A transient short-circuit fault occurs in the transmission line between bus1 and bus 2 at $t = 2.0s$. The communication delay is still assumed as $\tau_{12} = 200ms$.

After the fault is cleared, according to the proposed assessment index, the DER 1 and DER 2 units still need to execute the control mode 2. Similarly, the control performance regarding bus1 and bus2 voltages is shown in Figs. 9 (a) and (b) by using the control mode 1, in Figs.9 (c) and (d) by means of the proposed control mode 2, and in Figs.9 (e) and (f) under the compared distributed control [11].

From Figs. 9(a)-(d), it can be observed that by means of the control mode 2, the bus1 and bus2 voltages are controlled within the secure range of [0.95p.u., 1.05p.u.] even if on the initial stage of fault occurrence. Moreover, about after $t = 4.5s$, the voltage deviation between the two buses is completely eliminated. On the contrary, by using only local controller, the two bus voltages are not able to be stabilized within the secure range. Form Figs. 9(e) and (f), it can be seen that, when the distributed control [11] is used, the two bus voltages present larger fluctuation on the initial stage of fault occurrence. They are ultimately settled down, but there is a litter voltage deviation between the two buses. The comparative simulation results above indicate that the proposed distributed coordinated control still ensures the best control performance when encountered with a severe disturbance.

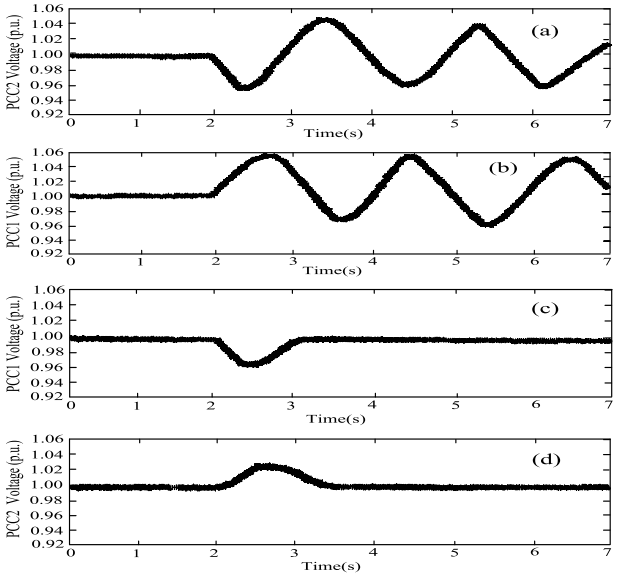

FIGURE 10. Control performance of bus voltages in Case 3. (a) bus1 voltage under the distributed control [11]; (b) bus2 voltage under the distributed control [11]; (c) bus1 voltage in the proposed control mode 2; (d) bus2 voltage in the proposed control mode 2.

C. CASE 3

The communication delay is assumed as $\tau_{12} = 2s$. The load changes are same as those in case 1. By using the compared distributed control [11], the control performance regarding bus1 and bus2 voltages is shown in Figs. 10(a) and (b). Compared with the previous results in Figs. 8(e) and (f) with the communication delay $\tau_{12} = 200ms$, the two bus voltages in Figs. 10(a) and (b) have much more severe fluctuations, since the larger communication delay leads to an incorrect voltage shift in the improved droop control. Figs.10(c) and (d) shows the control performance in the proposed control mode 2. It can be seen that the two bus voltages have no obvious changes in comparison with the previous results in Figs.8(c) and (d) with the communication delay $\tau_{12} = 200ms$. The reason is that the proposed delay-dependent robust control method can guarantee system robust stabilization, only if the communication delays do not exceed the allowable maximum upper bound.

D. CASE 4

A communication failure occurs between the 1st and the 3th second-level agents at $t = 2.0s$. The load changes are also same as those in case 1. By using the proposed control mode 2, the control performance regarding bus1 and bus2 voltages is shown in Figs.11 (a) and (b). It can be observed that the two bus voltages present only slightly larger fluctuation in comparison with the previous results in Figs. 8(c) and (d). It implies that the communication failure between the 1st and the 3th second-level agents does not deteriorate the control performance regarding bus 1 and bus 2 voltages. The reason is that the MAS based distributed coordinated control scheme has strong robustness to the effect of communication failures on the whole control functionality.

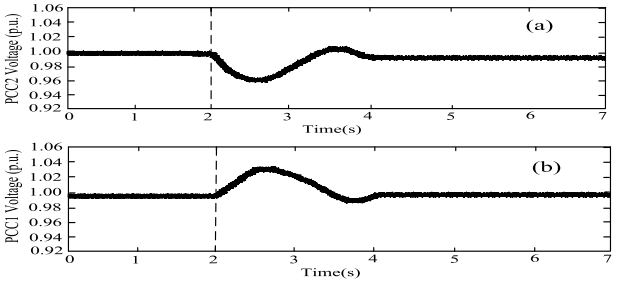

FIGURE 11. Control performance of bus voltages in Case 4. (a) bus1 voltage in the proposed control mode 2; (b) bus2 voltage in the proposed control mode 2.

From the above simulation results, it can be concluded that the MAS based distributed coordinated control improves the bus voltage performance when encountered with load demand changes, a severe fault disturbance, different communication delays and a communication failure.

VI. CONCLUSION

This paper develops a distributed coordinated control approach based on two-level MAS for DC ring-bus MGs. As opposed to the conventional hierarchical control approach, it does not require a central controller that depends on global information. The distributed coordinated control for each DER unit is built by the local controller combining with the coordinated control laws. To reduce communication pressure and enhance reliability, the coordinated control laws are synthesized by only using the states from neighboring second-level agents. Furthermore, an assessment index is proposed to assess whether each DER unit is necessary to implement the distributed coordinated control. To avoid that communication delays might deteriorate control performances, a delay-dependent robust control method is effectively applied into the control field of MGs to design the distributed coordinated controller.

The simulation results show that the better voltage performance has been achieved by means of the proposed method. The MAS based distributed coordinated control scheme can be applied to different DC ring-bus MGs by extending the control function of the agents or creating additional agents.

APPENDIX A PROOF OF THEOREM 4.1

Define a Lyapunov function for the system (11) as

$V_1(t) = \hat{\boldsymbol{x}}_1^T(t)\boldsymbol{P}_1\hat{\boldsymbol{x}}_1(t)$, where $\boldsymbol{P}_1 = \boldsymbol{P}_1^T > 0$.

Then, it is easy to obtain

$$\begin{aligned}
&\int_0^{t_f} [(\boldsymbol{x}_1(t) - \boldsymbol{x}_{r1}(t))^T \boldsymbol{Q}_1 (\boldsymbol{x}_1(t) - \boldsymbol{x}_{r1}(t))]dt \\
&= \int_0^{t_f} \hat{\boldsymbol{x}}_1^T(t)\hat{\boldsymbol{Q}}_1\hat{\boldsymbol{x}}_1(t)dt \\
&= \hat{\boldsymbol{x}}_1^T(0)\boldsymbol{P}_1\hat{\boldsymbol{x}}_1(0) - \hat{\boldsymbol{x}}_1^T(t_f)\boldsymbol{P}_1\hat{\boldsymbol{x}}_1(t_f) \\
&\quad + \int_0^{t_f} \{\hat{\boldsymbol{x}}_1^T(t)\hat{\boldsymbol{Q}}_1\hat{\boldsymbol{x}}_1(t) + \frac{d}{dt}(\hat{\boldsymbol{x}}_1^T(t)\boldsymbol{P}_1\hat{\boldsymbol{x}}_1(t))\}dt
\end{aligned}$$

$$\leq \hat{\boldsymbol{x}}_1^T(0)\boldsymbol{P}_1\hat{\boldsymbol{x}}_1(0) + \int_0^{t_f} \{\hat{\boldsymbol{x}}_1^T(t)\hat{\boldsymbol{Q}}_1\hat{\boldsymbol{x}}_1(t) + \dot{\hat{\boldsymbol{x}}}_1^T(t)\boldsymbol{P}_1\hat{\boldsymbol{x}}_1(t) + \hat{\boldsymbol{x}}_1^T(t)\boldsymbol{P}_1\dot{\hat{\boldsymbol{x}}}_1(t)\}dt$$

$$= \hat{\boldsymbol{x}}_1^T(0)\boldsymbol{P}_1\hat{\boldsymbol{x}}_1(0) + \int_0^{t_f} \left\{\begin{bmatrix}\hat{\boldsymbol{x}}_1(t)\\ \boldsymbol{\omega}_1(t)\end{bmatrix}^T \begin{bmatrix}\hat{\boldsymbol{A}}_1^T\boldsymbol{P}_1 + \boldsymbol{P}_1\hat{\boldsymbol{A}}_1 + \hat{\boldsymbol{Q}}_1 & \boldsymbol{P}_1\hat{\boldsymbol{D}}_1\\ \hat{\boldsymbol{D}}_1^T\boldsymbol{P}_1 & -\rho_1^2\boldsymbol{I}\end{bmatrix}\begin{bmatrix}\hat{\boldsymbol{x}}_1(t)\\ \boldsymbol{\omega}_1(t)\end{bmatrix} + \rho_1^2\boldsymbol{\omega}_1(t)^T\boldsymbol{\omega}_1(t)\right\}dt.$$

According to the above inequality, it is easy to deduce that, if the inequality (14) is satisfied, the tracking control system (11) of the 1st DER unit is asymptotically stable with the H_∞ control performance in (13) for $\forall \boldsymbol{\omega}_1(t)$. The proof is completed.

APPENDIX B PROOF OF THEOREM 4.2

Define a delay-dependent Lyapunov function for the tracking control system (21) as

$$V(t) = V_1(t) + V_2(t) + V_3(t),$$

where $V_1(t) = \tilde{\boldsymbol{x}}^T(t)\boldsymbol{P}\tilde{\boldsymbol{x}}(t)$, $V_2(t) = \int_{t-\bar{\tau}}^{t} \tilde{\boldsymbol{x}}^T(\tau)\boldsymbol{S}\tilde{\boldsymbol{x}}(\tau)d\tau$,

$$V_3(t) = \int_{-\bar{\tau}}^{0}\int_{t+\beta}^{t} \dot{\tilde{\boldsymbol{x}}}^T(\alpha)\boldsymbol{Z}\dot{\tilde{\boldsymbol{x}}}(\alpha)d\alpha d\beta,$$

$\boldsymbol{P}, \boldsymbol{S}, \boldsymbol{Z}$ are symmetric positive definite weighting matrices.

The derivative of $V_1(t)$ along the trajectory of system (21) satisfies that

$$\dot{V}_1(t) = 2\tilde{\boldsymbol{x}}^T(t)\boldsymbol{P}(\tilde{\boldsymbol{A}} + \widehat{\boldsymbol{A}})\bar{\boldsymbol{x}}(t) - 2\tilde{\boldsymbol{x}}^T(t)\boldsymbol{P}\widehat{\boldsymbol{A}} \int_{t-\bar{\tau}}^{t} \dot{\tilde{\boldsymbol{x}}}(\alpha)d\alpha + 2\tilde{\boldsymbol{x}}^T(t)\boldsymbol{P}\tilde{\boldsymbol{D}}\tilde{\boldsymbol{\omega}}(t).$$

By using Lemma [20], it is easy to obtain

$$\dot{V}_1(t) \leq \{\tilde{\boldsymbol{x}}^T(t)(\boldsymbol{P}\tilde{\boldsymbol{A}} + \tilde{\boldsymbol{A}}^T\boldsymbol{P} + \bar{\tau}\boldsymbol{X} + \boldsymbol{Y} + \boldsymbol{Y}^T\}\tilde{\boldsymbol{x}}(t) - 2\tilde{\boldsymbol{x}}^T(t)(\boldsymbol{Y} - \boldsymbol{P}\widehat{\boldsymbol{A}})\tilde{\boldsymbol{x}}(t-\bar{\tau}) + \int_{t-\bar{\tau}}^{t} \dot{\tilde{\boldsymbol{x}}}^T(\alpha)\boldsymbol{Z}\dot{\tilde{\boldsymbol{x}}}(\alpha)d\alpha + 2\tilde{\boldsymbol{x}}^T(t)\boldsymbol{P}\tilde{\boldsymbol{D}}\tilde{\boldsymbol{\omega}}(t)\}.$$

Then, it can be obtained that

$$\int_0^{t_f} \tilde{\boldsymbol{x}}^T(t)\tilde{\boldsymbol{Q}}\tilde{\boldsymbol{x}}(t)dt$$

$$= V(0) - V(t_f) + \int_0^{t_f} \{\tilde{\boldsymbol{x}}^T(t)\tilde{\boldsymbol{Q}}\tilde{\boldsymbol{x}}(t) + \dot{V}(t)\}dt$$

$$\leq V(0) + \int_0^{t_f} \{\tilde{\boldsymbol{x}}^T(t)(\tilde{\boldsymbol{Q}} + \boldsymbol{S} + \boldsymbol{P}\tilde{\boldsymbol{A}} + \tilde{\boldsymbol{A}}^T\boldsymbol{P} + \bar{\tau}\boldsymbol{X} + \boldsymbol{Y} + \boldsymbol{Y}^T)\tilde{\boldsymbol{x}}(t) - 2\tilde{\boldsymbol{x}}^T(t)(\boldsymbol{Y} - \boldsymbol{P}\widehat{\boldsymbol{A}})\tilde{\boldsymbol{x}}(t-\bar{\tau}) + 2\tilde{\boldsymbol{x}}^T(t)\boldsymbol{P}D\tilde{\boldsymbol{\omega}}(t) - \tilde{\boldsymbol{x}}^T(t-\bar{\tau})\boldsymbol{S}\tilde{\boldsymbol{x}}(t-\bar{\tau}) + \bar{\tau}\dot{\tilde{\boldsymbol{x}}}^T(t)\boldsymbol{Z}\dot{\tilde{\boldsymbol{x}}}(t) + \rho^2\tilde{\boldsymbol{\omega}}^T(t)\tilde{\boldsymbol{\omega}}(t) - \rho^2\tilde{\boldsymbol{\omega}}^T(t)\tilde{\boldsymbol{\omega}}(t)\}dt$$

$$= V(0) + \int_0^{t_f} \left\{\begin{bmatrix}\tilde{\boldsymbol{x}}(t)\\ \tilde{\boldsymbol{x}}(t-\bar{\tau})\\ \tilde{\boldsymbol{\omega}}(t)\end{bmatrix}^T \left\{\begin{bmatrix}\Theta & \boldsymbol{P}\widehat{\boldsymbol{A}} - \boldsymbol{Y} & \boldsymbol{P}\tilde{\boldsymbol{D}}\\ * & -\boldsymbol{S} & 0\\ * & * & -\rho^2\end{bmatrix} + \bar{\tau}\begin{bmatrix}\tilde{\boldsymbol{A}}\\ \widehat{\boldsymbol{A}}\\ \tilde{\boldsymbol{D}}\end{bmatrix}^T \boldsymbol{Z}\begin{bmatrix}\tilde{\boldsymbol{A}}\\ \widehat{\boldsymbol{A}}\\ \tilde{\boldsymbol{D}}\end{bmatrix}\right\}\begin{bmatrix}\tilde{\boldsymbol{x}}(t)\\ \tilde{\boldsymbol{x}}(t-\bar{\tau})\\ \tilde{\boldsymbol{\omega}}(t)\end{bmatrix} + \rho^2\tilde{\boldsymbol{\omega}}^T(t)\tilde{\boldsymbol{\omega}}(t)\right\}dt$$

According to the above inequality, by using Schur complement, it is easy to deduce that, if the inequality (23) holds, the system (21) is asymptotically stable with the H_∞ performance in (22). This completes the proof.

REFERENCES

[1] A. Kwasinski, "Quantitative evaluation of dc microgrids availability: Effects of system architecture and converter topology design choices," *IEEE Trans. Power Electron.*, vol. 26, no. 3, pp. 835–851, Apr. 2011.

[2] Q. Shafiee, T. Dragicevic, J. C. Vasquez, and J. M. Guerrero, "Hierarchical control for multiple DC-microgrids clusters," *IEEE Trans. Energy Convers.*, vol. 29, no. 4, pp. 922–933, Apr. 2014.

[3] A. T. Elsayed, A. A. Mohamed, and O. A. Mohammed, "DC micro-grids and distribution systems: An overview," *Electr. Power Syst. Res.*, vol. 119, pp. 407–417, Sep. 2015.

[4] A. Khorsandi, M. Ashourloo, and H. Mokhtari, "A decentralized control method for a low-voltage DC microgrid," *IEEE Trans. Energy Convers.*, vol. 29, no. 4, pp. 793–801, Apr. 2014.

[5] Y. J. Gu, X. Xiang, W. H. Li, and X. N. He, "Mode-adaptive decentralized control for renewable DC microgrid with enhanced reliability and flexibility," *IEEE Trans. Power Electron.*, vol. 29, no. 9, pp. 5072–5080, Sep. 2013.

[6] J. M. Guerrero, J. C. Vasquez, J. Matas, J. G. de Vicuna, and M. Castil-la, "Hierarchical control of droop-controlled AC and DC microgrids—A general approach toward standardization," *IEEE Trans. Ind. Electron.*, vol. 58, no. 1, pp. 158–172, Feb. 2011.

[7] X. Lu, J. M. Guerrero, K. Sun, J. C. Vasquez, R. Teodorescu, and L. Huang, "Hierarchical control of parallel AC-DC converter interfaces for hybrid microgrids," *IEEE Trans. Smart Grid*, vol. 5, no. 2, pp. 683–692, Mar. 2014.

[8] J. M. Guerrero, L. P. Chiang, T. L. Lee, and M. Chandorkar, "Advanced control architectures for intelligent microgrids—Part II: Power quality, energy storage, and AC/DC Microgrids," *IEEE Trans. Ind. Electron.*, vol. 60, no. 4, pp. 1263–1270, Apr. 2013.

[9] Q. Shafiee, J. M. Guerrero, and J. C. Vasquez, "Distributed secondary control for Islanded microgrids—A novel approach," *IEEE Trans. Power Electron.*, vol. 29, no. 2, pp. 1018–1031, Feb. 2014.

[10] Q. Shafiee, C. Stefanović, T. Dragičević, P. Popovski, J. Vasquez, and J. M. Guerrero, "Robust networked control scheme for distributed secondary control of Islanded microgrids," *IEEE Trans. Ind. Electron.*, vol. 60, no. 10, pp. 5363–5374, Oct. 2014.

[11] S. Anand, B. G. Fernandes, and J. M. Guerrero, "Distributed control to ensure proportional load sharing and improve voltage regulation in low-voltage DC microgrids," *IEEE Trans. Power Electron.*, vol. 28, no. 4, pp. 1900–1913, Apr. 2013.

[12] A. Bidram, A. Davoudi, F. L. Lewis, and J. M. Guerrero, "Distributed cooperative secondary control of microgrids using feedback linearization," *IEEE Trans. Power Syst.*, vol. 28, no. 3, pp. 3462–3470, Aug. 2013.

[13] V. Nasirian, S. Moayedi, A. Davoudi, and F. L. Lewis, "Distributed cooperative control for DC microgrid," *IEEE Trans. Power Electron.*, vol. 30, no. 4, pp. 2288–2303, Apr. 2015.

[14] C. Balarko, M. Rajat, and C. P. Bikash, "Wide-area measurement- based stabilizing control of power system considering signal transmission delay," *IEEE Trans. Power Syst.*, vol. 19, no. 4, pp. 1971–1979, Apr. 2004.

[15] T. Logenthiran, D. Srinivasan, and A. M. Khambadkone, "Multi-agent system for energy resource scheduling of integrated microgrids in a distributed system," *Electr. Power Syst. Res.*, vol. 81, no. 1, pp. 138–148, 2011.
[16] J. Lagorse, D. Paire, and A. Miraoui, "A multi-agent system for energy management of distributed power sources," *Renew. Energy*, vol. 35, pp. 174–182, Sep. 2010.
[17] C. X. Dou, D. Yue, J. M. Guerrero, X. P. Xie, and S. L. Hu, "Multiagent-system based distributed coordinated control for radial DC microgrid considering transmission time delays," *IEEE Trans. Smart Grid*, to be published, doi: 10.1109/TSG.2016.2524688.2016.
[18] S. Riverso, F. Sarzo, and G. Ferrari-Trecate, "Plug-and-play voltage and frequency control of islanded microgrids with meshed topology," *IEEE Trans. Smart Grid*, vol. 6, no. 3, pp. 1176–1184, May 2015.
[19] C. X. Dou, Z. S. Duan, and X. B. Jia, "Delay-dependent H∞ robust control for large power systems based on two-level hierarchical decentralized coordinated control structure," *Int. J. Syst. Sci.*, vol. 42, no. 1, pp. 201–217, 2013.
[20] Y. S. Lee, Y. S. Moon, W. H. Kwon, and P. G. Park, "Delay-dependent robust H∞ control for uncertain systems with a state-delay," *Automatica*, vol. 40, no. 1, pp. 65–72, 2004.

CHUNXIA DOU received the B.S. and M.S. degrees in automation from the Northeast Heavy Machinery Institute, Qiqihaer, China, in 1989 and 1994, respectively, and the Ph.D. degree from the Institute of Electrical Engineering, Yanshan University, Qinhuangdao, China, in 2005. In 2010, he joined the Department of Engineering, Peking University, Beijing, China, where he was a Post-Doctoral Fellow for two years. Since 2005, he has been a Professor with the Institute of Electrical Engineering, Yanshan University. Her current research interests include multi-agent-based control, event-triggered hybrid control, distributed coordinated control, and multi-mode switching control and their applications in power systems, microgrids, and smart grids.

DONG YUE (SM'08) received the Ph.D. degree from the South China University of Technology, Guangzhou, China, in 1995. He is currently a Professor and the Dean of the Institute of Advanced Technology, Nanjing University of Posts and Telecommunications, and also a Changjiang Professor with the Department of Control Science and Engineering, Huazhong University of Science and Technology. Up to now, he has authored over 100 papers in international journals, domestic journals, and international conferences. His research interests include analysis and synthesis of networked control systems, multi-agent systems, optimal control of power systems, and Internet of things. He is currently an Associate Editor of the IEEE Control Systems Society Conference Editorial Board and also an Associate Editor of the IEEE TRANSACTIONS ON NEURAL NETWORKS AND LEARNING SYSTEMS, the *Journal of the Franklin Institute*, and the *International Journal of Systems Science*.

ZHANQIANG ZHANG received the dual B.S. degrees in electrical engineering and automation/mathematics and applied mathematics from the Hebei University of Science and Technology, Shijiazhuang, China, in 2015. He is currently pursuing the M.S. degree in automation with Yanshan University, Qinhuangdao, China. His current research interests include microgrids and distributed generation technology.

JOSEP M. GUERRERO (S'01–M'04–SM'08–FM'15) received the B.S. degree in telecommunications engineering, the M.S. degree in electronics engineering, and the Ph.D. degree in power electronics from the Technical University of Catalonia, Barcelona, in 1997, 2000, and 2003, respectively. Since 2011, he has been a Full Professor with the Department of Energy Technology, Aalborg University, Denmark, where he is currently responsible for the Microgrid Research Program. Since 2012, he has been a Guest Professor with the Chinese Academy of Science and the Nanjing University of Aeronautics and Astronautics. Since 2014, he has been a Chair Professor with Shandong University. Since 2015, he has been a Distinguished Guest Professor with Hunan University.

His research interests is oriented to different microgrid aspects, including power electronics, distributed energy-storage systems, hierarchical and cooperative control, energy management systems, and optimization of microgrids and islanded microgrids; recently specially focused on maritime microgrids for electrical ships, vessels, ferries, and seaports. In 2015, he was elevated as an IEEE Fellow for his contributions on distributed power systems and microgrids. He received the Best Paper Award of the IEEE TRANSACTIONS ON ENERGY CONVERSION for the period 2014–2015. He was the Chair of the Renewable Energy Systems Technical Committee of the IEEE Industrial Electronics Society. He is an Associate Editor of the IEEE TRANSACTIONS ON POWER ELECTRONICS, the IEEE TRANSACTIONS ON INDUSTRIAL ELECTRONICS, and the *IEEE Industrial Electronics Magazine*, and an Editor of the IEEE TRANSACTIONS ON SMART GRID and the IEEE TRANSACTIONS ON ENERGY CONVERSION. He has been a Guest Editor of the IEEE TRANSACTIONS ON POWER ELECTRONICS Special Issues: Power Electronics for Wind Energy Conversion and Power Electronics for Microgrids; the IEEE TRANSACTIONS ON INDUSTRIAL ELECTRONICS Special Sections: Uninterruptible Power Supplies systems, Renewable Energy Systems, Distributed Generation and Microgrids, and Industrial Applications and Implementation Issues of the Kalman Filter; and the IEEE TRANSACTIONS ON SMART GRID Special Issue on Smart dc Distribution Systems. In 2014 and 2015, he was awarded by Thomson Reuters as a Highly Cited Researcher.